Available online at **www.joac.info**

ISSN: 2278-1862

Journal of Applicable Chemistry

2020, 9 (2): 229-239

(International Peer Reviewed Journal)

Novel Sphere CuO/Ag_3PO_4 Nanocomposites with Enhanced Visible Light Photocatalytic Activity for Degradation of Amaranth

K. Palpandi[1], K. Eswaran[2] and B. Kavitha[1]*

1. P.G and Research Department of Chemistry, Cardamom Planter's Association College, Bodinayakanur, Tamil nadu-625513, **INDIA**
2. Department of Chemistry, College of Natural Sciences, Kongju National University, Gongju, Chungnum 32588, **SOUTH KOREA**

Email: kaviravee@gmail.com

Accepted on 27th February, 2020

ABSTRACT

Novel CuO/Ag_3PO_4 nanocomposites have been synthesized via co-precipitation approach and characterized by means of X-ray powder diffraction (XRD), scanning electron microscopy (SEM), energy dispersive X-ray spectroscopy (EDS), Fourier transform infrared spectroscopy (FT-IR), transmission electron microscopy (TEM) and UV-visible diffuse reflectance spectra (UV-Vis-DRS). The as prepared CuO/Ag_3PO_4 has a monoclinic structure with average crystalline size of 25.4 nm. The SEM outcomes suggest that the CuO/Ag_3PO_4 has sphere like structure reveals strong absorption in visible region and it suggests exceedingly great photocatalytic activity for the photodegradation of amaranth under visible light irradiation. The possible mechanism for the extraordinary overall performance of sphere like CuO/Ag_3PO_4 nanocomposites is proposed. The photocatalytic pastime enhancement of CuO/Ag_3PO_4 is related to the efficient separation of electron hole pairs. The impact on various response parameters just like the effect of catalyst concentration, preliminary amaranth concentration, pH and contact time were investigated in detail.

Graphical Abstract

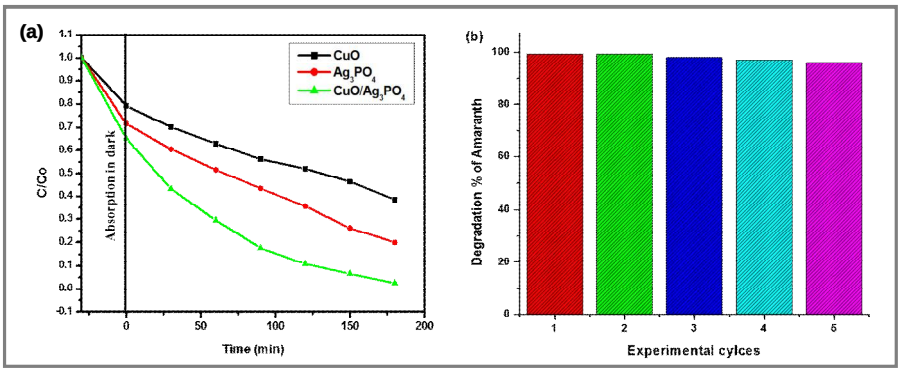

(a) photodegradation curve of amaranth in the presence of CuO, Ag_3PO_4, CuO/Ag_3PO_4under visible light irradiation and (b) Reusability of CuO/Ag_3PO_4 for the photodegradation of amaranth.

Keywords: $CuO/AgPO_4$ nanosphere, Photocatalytic activity, Visible light, Amaranth.

INTRODUCTION

In the latest year, semiconductor photocatalysis have attracted an awful lot attention; specifically photocatalysis which are surprisingly reactive under plentiful sun light have shown a huge range of utility from water disinfection, removal and degradation of organic pollutants [**1-3**]. Nevertheless, semiconductor substances available so far in large part restrained through both deficient charge separation capability of poor photocatalytic efficient in the visible light region [**4-5**]. To deal with the problems, plenty of attempts have targeting on exploring and fabricating novel material with extraordinarily efficient in the visible light region for photocatalytic application [**6-9**].

Copper (II)-oxide nanoparticles (CuO-NPs) belongs to monoclinic structure device. It has wide variety of applications in line with the physical and chemical properties, together with superconductivity, photovoltaic residences, distinctly strong, low cost and the antimicrobial activity. Therefore it's far very important to increase powerful method to enhance the steadiness of the CuO photocatalysts. However, CuO shows the photocatalytic ability under ultraviolet (UV) irradiation, which limits the use of natural sun light for the strength of UV light occupies much less than 5% in that of all of the solar light. To improve the usage of sun power within the photocatalyst of CuO, numerous techniques, inclusive of coupling with metal oxide and metal phosphate, were followed to enhance photocatalytic performance [**10**]. Much work has been done on photocatalytic substances that are sensitive within the visible light region. The Ag_3PO_4 (indirect band gap of 2.36 eV as well as a direct band gap of 2.43 eV) [**11**] has been recognized as one of the most efficient visible light driven photocatalysts because of its brilliant photooxidation capabilities for organic dye decomposition [**12**].

Recently many works related to the combination of $Ag_3PO_4$with distinct materials, which include AgX (X=Cl, Br and I) [**13**], Fe_3O_4 [**14**], TiO_2, SnO_2 [**15**], and GO [**16**] were exploited to enhance the stableness and activity. However, synthesis and photocatalytic property of CuO/Ag_3PO_4 nanocomposites have not yet been mentioned even though they are associated with the shape controlling preparation technique. The substances have been received the use of co-precipitation and impregnation techniques, and the overall performance changed into evaluated for the photcatalytic degradation of amaranth in the photocatalytic system using visible light radiation.

The amaranth is commonly used for coloring agent in fabric substances, paper, leather and wooden and many others. Although, for long time this dye was used as food coloring agent in jams, jellies, cake and ketchup. However, latest years it is legal prohibition in many countries because of the carcinogenicity and other poisonous effects of amaranth. It is now properly installed that a extend consumption of amaranth can result to tumors, allergy, respiration troubles and delivery defects [**17**]. The common chemical treatments have been failed for elimination of amaranth because of their suitable solubility nature in water. Commonly, organic cardio waste water remedy gadget additionally ineffective for decolorisation of majority of dyes [**18**]. For that reason, develop oxidation procedure inclusive of photocatlytic experiment has been effectively used by many people [**19**].

The goal of this work is to examine the phase, microstructure morphology and textural properties of CuO/Ag_3PO_4 by X-ray powder diffraction, scanning electron microscopy (SEM), UV-Visible diffuse reflectance spectra (UV-Vis-DRS), Fourier transform infrared spectroscopy (FT-IR) and transmission electron microscopy (TEM). The photocatalytic activity of the as synthesized nanosphere of CuO/Ag_3PO_4 was examined, for degradation of amaranth below visible light irradiation.

MATERIALS AND METHODS

Chemicals and Materials: All chemical substances had been bought from Merck. The chemicals used were of analytical grade and implemented without in additional purification. Double distilled water was used in all photodegradation experiments**.**

Synthesis of photocatalyst (CuO/Ag_3PO_4): Initially CuO was prepared from, aqueous solution of copper acetate (0.02 mol) in round bottom flask. 1 ml glacial acetic acid is delivered to above aqueous solution and heated to a 100°C with constant stirring. About 0.4 g of NaOH is added to above heated solution till pH reaches to 6-7. The huge quantity of black precipitate is formed right now. It is centrifuged and washed several instances with double distilled water. The acquired precipitate has become dried in air for 24 h.

Ag_3PO_4 was prepared by the simple co-precipitation method. In a typical synthesis, aqueous citric acid solution (50 mL, 0.1 M) was introduced drop wise into $AgNO_3$ aqueous solution (50 mL, 0.05 M) in a beaker, the mixture was stirred for 50 min in order to obtain a clear solution. The aqueous Na_2HPO_4 solution (15 mL, 0.02 M) was added drop wise to the above mixture; the reaction mixture was sealed and kept stirring for additional 2 h. The obtained precipitate was collected by centrifugation, washed several times with absolute ethanol and distilled water and finally dried at 60°C in an air hot oven.

In a typical synthesis of CuO/Ag_3PO_4, 5 g of CuO and 1.3142 g of Ag_3PO_4 was dispersed in 50 mL of ethanol and sonicated for 30 min. The whole suspension was refluxed for 2 h and kept stirred for 2 h. The CuO/Ag_3PO_4 photocatalyst was then filtered, washed and dried in an air hot oven for 120°C and calcinated at 500°C.

Characterization: The photocatalyst were characterized via the following techniques. The UV–Vis diffuse reflectance spectra had been acquired for dry-pressed disk samples the usage of a JASCO V-550 double beam spectrophotometer with PMT detector equipped with an integrating sphere assembly, the use of $BaSO_4$ as a reference sample. The spectra had been recorded at room temperature starting from 200 nm to 800 nm. Fourier Transform Infrared Spectrum (FT-IR) of synthesized photocatalyst was acquired the usage of Shimadzu Fourier Transform Infrared Spectrometer (IR Affinity-1) with KBr–nanoparticles combination in the form of pellets. The shape and structure of the photocatalyst were determined by means of X- ray powder diffraction with Cu Kα radiation at 25ºC using XPERT PRO X–RAY and the structural assignments were made close to the standard JCPDS powder diffraction files. Scanning electron microscopes (SEM) of the nanoparticles had been taken through a JM 6701F–6701 tool in each secondary and backscattered electron modes. The elemental evaluation changed into detected via an energy dispersive X-ray spectroscopy (EDX) connected to the SEM.

Measurement of photocatalytic activity: The photodegradation of amaranth became followed to evaluate the photocatalytic activity of CuO/Ag_3PO_4 in a photoreaction apparatus [**20**]. Photocatalytic experiments have been finished in an immersion type photoreactor. 300 mL of Amaranth with an initial concentration of 10 µM turned into taken in a cylindrical glass vessel, which changed into surrounded via a circulating water jacket to chill the lamp. Air changed into bubbled continuously into the aliquot with the aid of an air pump so as to offer a regular supply of dissolved oxygen. Before light irradiation the reaction mixture was stirred in dark for 30 min to gain the adsorption-desorption equilibrium between the catalyst and dye molecules. A 300 W Xe arc lamp with an ultraviolet cut off filter turned into used because the visible light irradiation source. During the course of light irradiation, 5 mL of aliquot was accrued at regular time interval of 30 min. Then the samples have been centrifuged to eliminate the photocatalyst and the filtrate became analyzed through UV–Visible spectrometer at λ_{max}= 520 nm. The photodegradation of Amaranth was calculated by means of the formulation given under:

$$\text{Photodegradation (\%)} = \frac{C_0 - C}{C_o} \qquad (1)$$

Where, C_0 is the concentration of Amaranth before irradiation time and C is the concentration of Amaranth after a certain irradiation time.

RESULTS AND DISCUSSION

UV-Vis-DRS: In order to analyze the band gap of CuO, Ag_3PO_4 and CuO/Ag_3PO_4 nanoparticles, the absorption spectra of synthesized CuO, Ag_3PO_4 and CuO/Ag_3PO_4 were tested by way of UV-Vis-DRS spectrophotometer and the results are shown in figure 1a. The pure Ag_3PO_4 confirmed an essential absorption at about 500 nm. The Ag_3PO_4/CuO samples showed improving in the visible region and the visible absorption intensity of the photocatalyst have been increased with the enhancing CuO content material because CuO became the good light absorptive material, the same result have been reported by means of Yu [21]. Meanwhile, it was observed that the color composite sample became almost black, whilst yellow Ag_3PO_4 added into the pure CuO photocatalyst. This result indicated that the photocatalyst may want to absorb extra photons. Therefore, it might be favorable for photocatalytic reaction. The band gap was calculated by way of Tauc's formula which suggests the relationship amongst coefficient and the incident photon energy of CuO. The Tauc's equation is supplied as beneath [22]:

$$\alpha h\nu = A(h\nu - E_g)^{\frac{n}{2}} \qquad (2)$$

Where α is the absorption coefficient. A is a constant and n relies upon on whether the transition semiconductor is indirect (n= 4) or direct (n=1). Accordingly, the plot $(\alpha h\nu)^2$ as a feature of hν has been displayed in figure 1b, The band gap energy can be extrapolating the linear absorption edge of the curve. The Eg of CuO, Ag_3PO_4 and CuO/Ag_3PO_4 microcrystal became determined to be 2.8, 2.36 and 1.22 eV respectively. These results indicated that CuO/Ag_3PO_4 has narrow band gap, which might be beneficial to enhancing the photocatalytic activity of the composites.

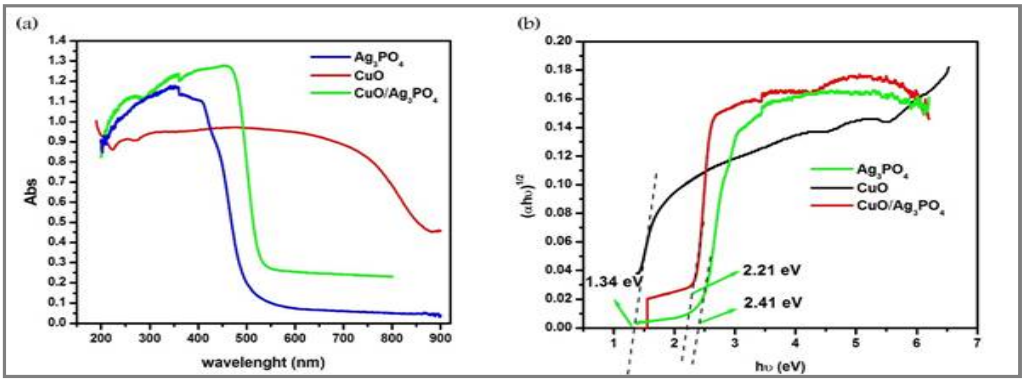

Figure 1. (a) UV-Vis-DRS of Ag_3PO_4 (blue), CuO (red), CuO/Ag_3PO_4 (green) (b) Tauc plot of Ag_3PO_4 (green), CuO (black), CuO/Ag_3PO_4 (red).

FT-IR: To certify the existence of interaction between CuO and Ag_3PO_4 nanoparticles. FT-IR spectra of CuO, the Ag_3PO_4 and CuO/Ag_3PO_4 had been tested and as compared in figure 2. The sharp peak found at 601 cm^{-1} in the spectrum of CuO nanoparticles is the characteristics of Cu-O bond formation. The broad absorption peaks at around 3430 cm^{-1} is due to the adsorbed water molecules. For the pure Ag_3PO_4 and the CuO/Ag_3PO_4 composites, a strong and wide absorption around 3200 cm^{-1} and sharp band at 1655 cm^{-1} have been found, which will be attribute to the stretching vibration of O–H and the bending vibration of H–O–H of water molecule respectively. An extensive absorption band centered at 1400 cm^{-1} originated from the stretching of the doubly bonded oxygen vibration (P=O) [23]. Two absorption bands at 1015 cm^{-1} and 550 cm^{-1} were also observed within the spectra, and these bands might be assigned to molecular vibrations of the phosphate (PO_4^{3-}) [24-29].

XRD: Figure 3 suggests XRD patterns of the as-synthesized samples. It is found that CuO has monoclinic structure (JCPDS no: 48-1548) whilst Ag_3PO_4 has cubic primitive phase (JCPDS no: 89-7399). In addition the CuO/Ag_3PO_4 hybrid nanoparticles exhibited a coexistence of each CuO and

Ag_3PO_4 phase. The exclusive pattern of CuO suggests peak at 35.38°, 38.6°, 48.66° and 53.33° that is correspond to (T11), (111), (202) and (020) planes [**30**] respectively. There after four sharp peaks at 29.7°, 33.4°, 36.6° and 42.5° which were accurate agreement with the diffraction shape from the 200, 210, 211 and 220 crystal plane of a body targeted cubic Ag_3PO_4 respectively.

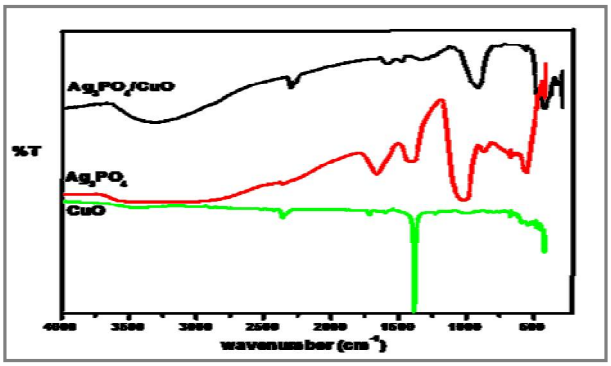

Figure 2. FT-IR spectra of CuO, Ag_3PO_4, Ag_3PO_4/CuO.

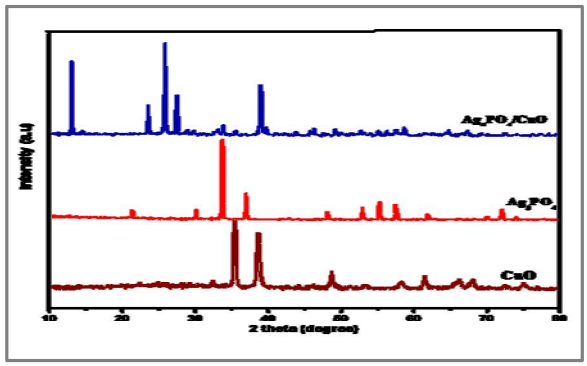

Figure 3. XRD pattern of CuO, Ag_3PO_4, Ag_3PO_4/CuO.

SEM, EDX and TEM: The morphology of the photocatalyst was tested by SEM and the micrographs are displayed in figure 4(a) indicates nanoflake like structure of CuO. Moreover, those nanoflakes are rough and uneven in surface. In figure 4 (b) shows olive ball like structure of Ag_3PO_4 and figure 4(c) nanocomposite are spherical like in form and barely agglomerated, favoring proper photocatalytic activity. TEM image of CuO/Ag_3PO_4 is depicted in Figure 4(d). The organized photocatalyst are flakes and microspheres, which is right agreement with the SEM results.

The existence of the silver phosphate at the surface of CuO became detected via EDX shown in figure 5(a), 5(b) and 5(c). The EDX information of the nanocomposites is given in table 1. The results revealed that all the elements (Ag, Cu, P and O) are really found at their corresponding keV values. The peaks due to Cu, O, Ag and P are present at 0.9 keV, 0.5 keV, 3.1 keV and 2.1 keV respectively.

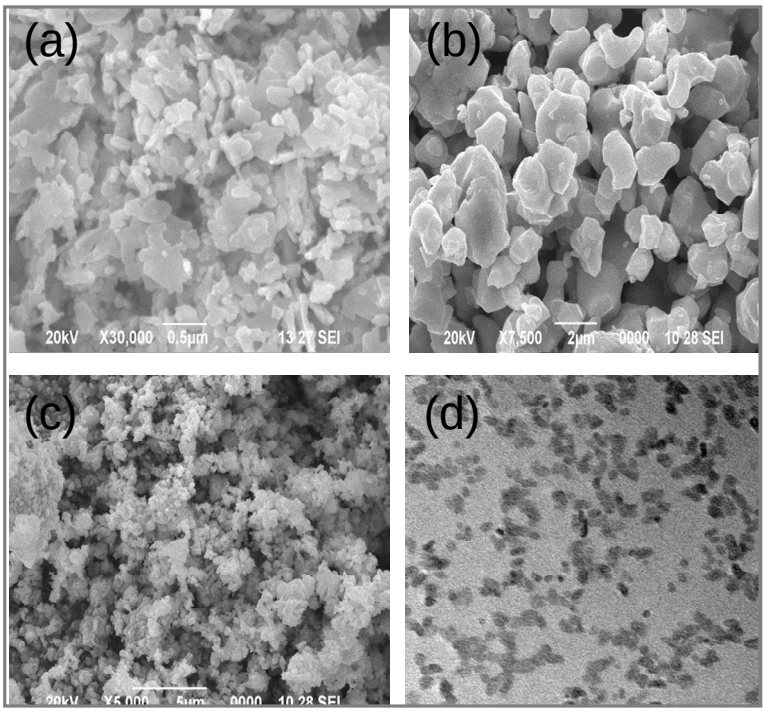

Figure 4. SEM image of (a) CuO, (b) Ag_3PO_4 (c) Ag_3PO_4/CuO and (d) TEM image of Ag_3PO_4/CuO.

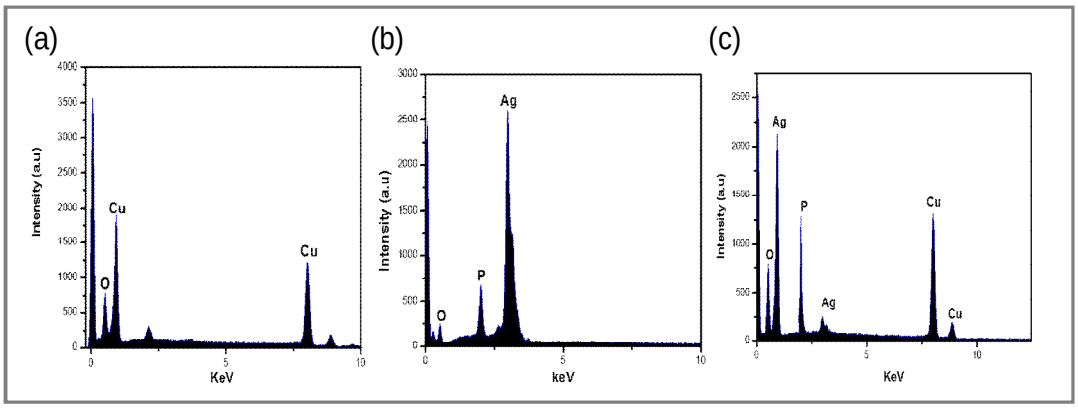

Figure 5. EDX specra of (a) CuO, (b) Ag_3PO_4 (c) Ag_3PO_4/CuO.

Table 1. EDX data of CuO, Ag_3PO_4 and CuO/Ag_3PO_4

Sample	Weight %	Atomic %	KeV
CuO	Cu = 78.49 O = 21.51	Cu = 52.12 O = 47.88	Cu = 2.14 O = 9.68
Ag_3PO_4	O = 21.01 P = 6.71 Ag = 72.27	O = 59.70 P = 9.85 Ag = 30.45	O = 0.53 P = 2.14 Ag =2.81
CuO/Ag_3PO_4	O = 25.30 Cu = 63.85 Ag = 4.85 P = 6.71	O =58.02 Cu= 30.48 Ag = 1.65 P = 9.85	O = 2.02 Cu = 15.09 Ag = 3.15 P = 2.14

Photocatalytic activity: The photocatalytic activities of the as prepared CuO, Ag_3PO_4 and CuO/Ag_3PO_4 are evaluated through detecting degradation of amaranth in an aqueous solution under visible light irradiation (λ>420 nm). A blank experiment with no catalyst demonstrated that no major change after irradiated for 30 min. Figure 6(a) indicates the photocatalytic degradation performance of amaranth turned into 43.7%, 57.0%, 99.3% for the pure Ag_3PO_4, CuO and CuO/Ag_3PO_4 were achieved in 180 min of visible light irradiation. The end result indicated that amaranth can be degraded greater for CuO/Ag_3PO_4 (99.3 %) than by the pure Ag_3PO_4.

The photocatalytic stability was evaluated via the cyclic degradation experiments. As proven in figure 6(b), the photocatalytic activity of the as-synthesized CuO/Ag_3PO_4 still keeps an excessive level, although it has been used 5 times. The result indicating that the prepared CuO/Ag_3PO_4 photocatalysts can shows a strong and efficient visible light irradiation.

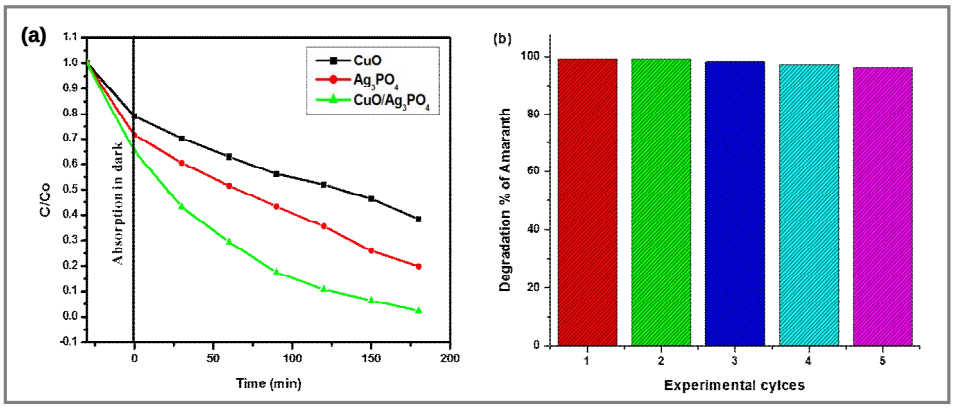

Figure 6(a). photodegradation curve of amaranth in the presence of CuO, Ag_3PO_4, CuO/Ag_3PO_4 under visible light irradiation and (b). Reusability of CuO/Ag_3PO_4 for the photodegradation of amaranth.

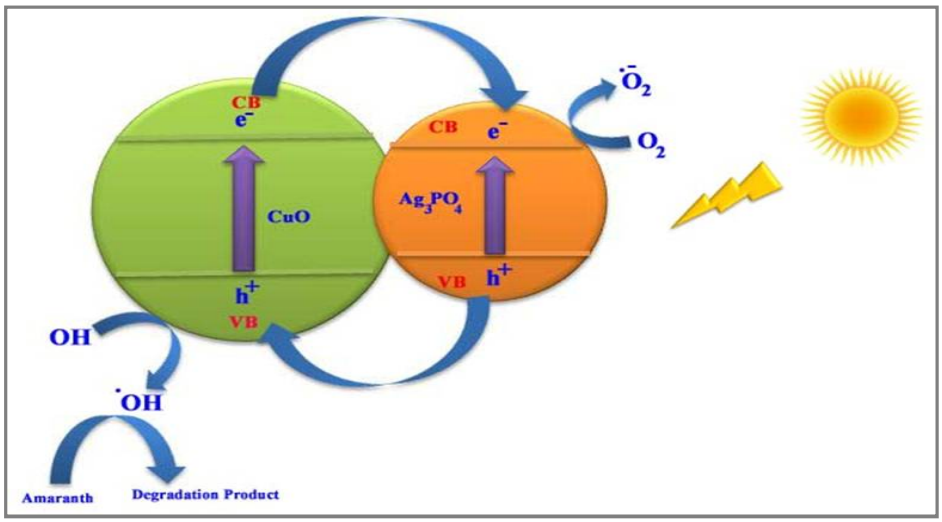

Figure 7. The schematic diagram of electron transfer in CuO/Ag_3PO_4 under visible light irradiation.

The possible mechanism of photocatalytic process: The photocatalytic mechanism was demonstrated in figure 7. From figure 7 it could be seen that under the visible light irradiation, Ag_3PO_4 changed into energized. Electron got exited to the Ag_3PO_4 conduction band, at that point the electron could be moved to the CuO underneath the effect of electrical field inside the composite body. Along these lines, it might retransfer to the floor of the CuO to take an interest inside the photocatalytic response. At that point, h^+ becomes left inside the valance band. In this manner, electron and holes could be adequately isolated all together that photocatalytic in general execution of the impetus changed into improved. The green switch of the electron may be attributed to the changed CuO, which were successful in electron hole pair partition. The fundamental energetic species inside the photocatalytic system were inspected inside the trial of in situ catch of dynamic species

$$CuO + h\nu \rightarrow CuO\ (h^+ + e^-) \quad (3)$$

$$CuO\ (e^-) + Ag_3PO_4 \rightarrow CuO + Ag_3PO_4\ (e^-) \quad (4)$$

$$Ag_3PO_4(e^-) + O_2 \rightarrow O_2^{\bullet -} + Ag_3PO_4 \quad (5)$$

$$O_2^{\bullet -} + h^+ + \text{amaranth} \rightarrow CO_2 + H_2O \quad (6)$$

Effect of pH: pH is an important factor that influences the photodegradation process. The effect of the pH is explained the surface charge properties of the photo-catalyst and therefore the adsorption behavior of pollutants. The photocatalytic degradation of amaranth has been studied in the pH range of 2-6 at a fixed catalyst dosage of CuO/Ag_3PO_4(0.125 g L^{-1}). The results are display in figure 8. The photo degradation increases from pH 2-4 and then decreases as the pH 6. It can observed that in more acidic form the dye will be predominantly in it is pronated form and surface will be positively charged. On other hand, the protonated form of the dye can strive with oxygen for the conduction band electron of the irradiated photocatalyst [**31**]. The results reveal (Figure 8) that, the dye molecules are easily absorb by positive charged CuO/Ag_3PO_4 surface at lower pH. The maximum photocatalytic degradation in present condition will be gradual drop of increase in pH, due to the mechanism for photocatalytic experiment may change from reductive to an oxidative one. Therefore, the increment of pH (pH 6) of dye was repulsed by negatively charged catalytic surface. Based on results of figure 8 as mentioned before, the enhancement of photodegradation of amaranth at pH 4 may be due to aggregation of charge on the outer surface of synthesized catalyst. So, the variation of pH can be affected the photocatalytic efficiency of coupled photocatalyst in the suspension.

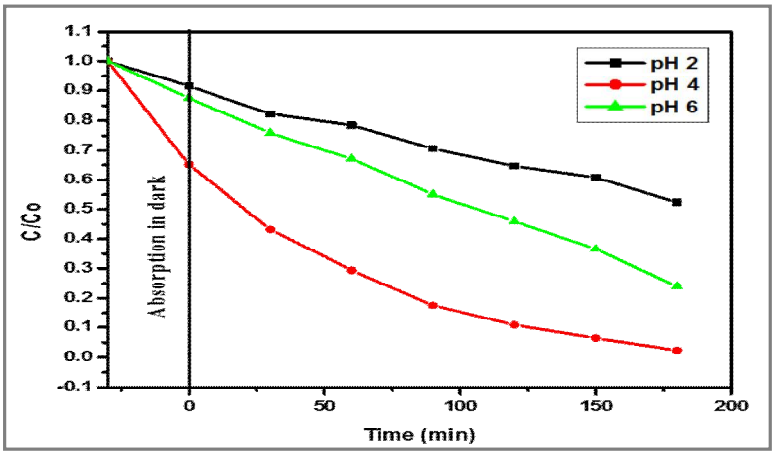

Figure 8. Effect of pH on photodegradation of amaranth.

Effect of catalyst dose: The effect of catalyst dosage on photodegradation of amaranth and obtain the optimum condition with respect to the amount of catalyst used at which the photodegradation efficiency is maximum that can save the unnecessary use of the excess of photo-catalyst quantity. The experiments were conducted with varying catalyst dosage (0.075 g L^{-1} to 0.15 g L^{-1}) of CuO/Ag_3PO_4 on the decomposition of the amaranth dye molecules during 180 min. of irradiation. It is observed that the efficiency increases up to 0.125 g L^{-1} of the dye, beyond which it shows a gradual decrease in degradation efficiency (Figure 9). This observation can be explained in terms of availability of active sites on the catalyst surface and the penetration of visible light into the suspension, this is possible to turn increases the rate of radical formation. At the same time, the surplus addition of the catalyst makes the solution more turbid and light penetration is retarded. The addition of surplus catalyst also results in the deactivation of activated molecules by collision with ground state molecules and hence the photoactive volume of suspension decreases.

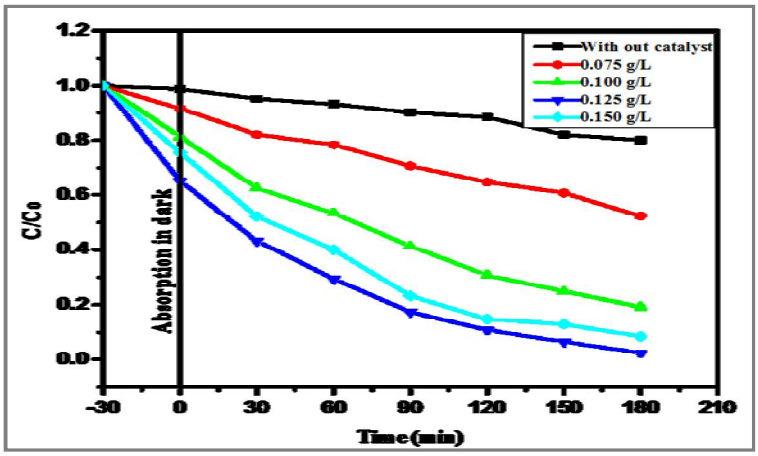

Figure 9. Effect of CuO/Ag_3PO_4 dosage on the photodegradation of amaranth.

Effect of initial dye concentration: Subsequently optimizing pH and catalyst dosage (pH4 and CuO/Ag_3PO_4 concentration 0.125 g L^{-1}), photocatalytic degradation was carried out by varying the initial dye concentration of amaranth from 6 µM to 12 µM. Figure 10 shows that photodegradation efficiency increases with increase in dye concentration up to 10 µM and further increase leads to decrease in degradation efficiency [**32**]. This can be explained by the following reason: the initial concentration of the dye increased, more dye molecules are absorbed onto the surface of the CuO surface. Unfortunately, the absorbed dye molecules are not degraded immediately due to the intensity of the light, the constant catalyst amount and less penetration efficiency. For that reason, increase in the dye concentration of the solution becomes more intense colored and the path length of the photons

entering the solution (according to Bee-Lambert's law) is decrease thereby fewer photons reached the catalyst surface. Hence competitive adsorption of O_2 and OH^- at the same sites decreases, meaning lower formation rate of $O_2^{\bullet-}$ and $^{\bullet}OH$ radicals, the principal oxidants necessary for high decolorization efficiency. Therefore, dye concentration also affects the color removal efficiency. Initial dye concentration provides an important driving force to overcome all mass transfer resistance of the dye between aqueous and solid phases.

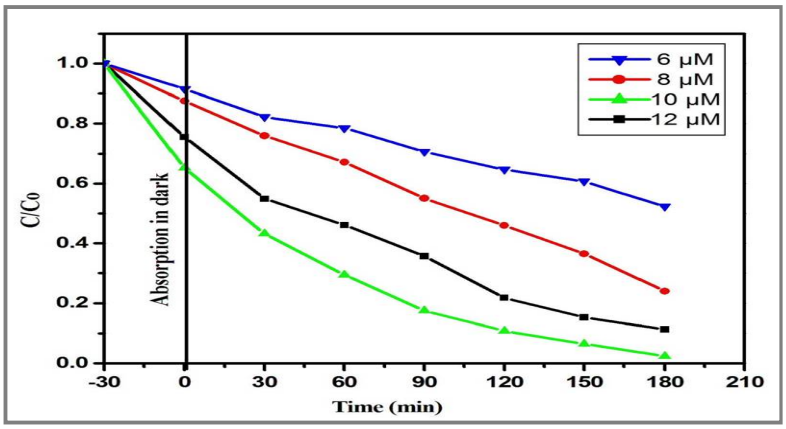

Figure 10. Effect of different amaranth concentration on its photodegradation.

APPLICATION

The nanocomposite can be potentially utilized as a suitable photocatalyst for removal of organic pollutants from environment.

CONCLUSION

CuO/Ag_3PO_4 nanocomposite with excellent visible light photocatalytic action was set up by chemical precipitation strategy and effectively described utilizing UV-Vis-DRS, XRD, SEM, TEM and EDX techniques. The most extreme level of amaranth photodegradation (99.30%) was accomplished with CuO/Ag_3PO_4 grouping of 0.125 g L^{-1}, initial amaranth concentration of 10 µM, pH 4 and illumination time of 180 min. additionally the nanocomposite is profoundly steady with expanded surface region and has greatest photocatalytic action for the Degradation of amaranth when contrasted with CuO and Ag_3PO_4. The nanocomposite is profoundly steady with expanded surface region and has greatest photocatalytic action for the Degradation of amaranth when contrasted with CuO and Ag_3PO_4.

ACKNOWLEDGEMENT

The authors are also thankful to the Management of C.P.A College for providing necessary laboratory facilities.

REFERENCES

[1]. Q. J. Xiang, J. G. Yu, M. Jaroniec, grapheme based semiconductor photocatalysis, *Chem. Soc. Rev.*, **2012**, 41 782-796.
[2]. H. Tong, S. X. Ouyang, Y.P. Bi, N. Umerzawa, M. Oshikiri, J. H. Ye, Nanophotocatalytic materials possibilities and challenges, *Adv. Mater,*. **2012**, 24, 229-251.
[3]. A. Kubacka, M. Fernandez-Garcia, G. Colon, Advanced nanoarchitectures for solar photocatalytic applications, *Chem. Rev,*. **2012**, 112, 1555-1614.

[4]. G. H. Tian, H. G. Fu, L. Q. Jing, B. F. Xin, K. Pan, Preparation and characterization of stable biphase TiO_2 photocatalyst with high crystallinity, large surface area, and enhanced photoactivity, *J.Phys. Chem.,* **2008**, 112, 3083-3089.
[5]. X. B. Chen, S. H. Shen, L. J. Guo, S. S .Mao, Semiconductor-based photocatalytic hydrogen generation, *Chem. Rev.*, **2010**, 110, 6503-70.
[6]. Z. G. Yi, J. H. Ye, N. Kikugawa, T. Kako, S. Ouyang, H. S. Williams, H. Yang, J. Y. Cao, W. J. Luo, Z. S. Li, R.L. Withers, on orthophosphate semiconductor with photooxidation properties under visible-light irradiation, *Nat. Mater.*, **2010**, 9, 559-564.
[7]. X. G. Ma, B. Lu, D. Li, R. Shi, C. S. Pan, Y. F. Zhu, origin of photocatalytic activation of silver orthophosphate from first-principles, *J. Phy. Chem. C,***2011**, 115, 4680-4687.
[8]. Jayesh Bhatt, Surbhi Benjamin, Rakshit Ameta, Suresh C. Ameta, Enhancement of Photodegradation of Picric Acid (2,4,6-Trinitrophenol) by Fabrication of Visible-Light-Active SnO_2 Quantum Dots/TiO_2 Nanospheres Composite, *J. Applicable Chem.*, **2019**, 8, 1805-1812.
[9]. K. K. Jat, J. Bhatt, S. C. Ameta, Photodegradation of Fast Green by Using SnO_2 Quantum Dots/TiO_2 Nanoparticles Composite, *J. Applicable Chem.*, **2019**, 8, 139-145.
[10]. X. F. Yang, H. Y. Cui, Y. Li, J .L. Qin, R. X. Zhang, H. Tang, Fabrication of Ag_3PO_4-graphene composites with highly efficient and stable visible light photocatalytic performance, *ACS Catal.*, **2013**, 3, 363-369.
[11]. P. Y. Dong, Y. H. Wang, H. H.Li, H. Li, X. L.Ma, L. L.Han, Shape-controllable synthesis and morphology-dependent photocatalytic properties of Ag_3PO_4 crystal, *J. Mater. Chem. A*, **2013**, 1, 4651-4656.
[12]. Y. Bi, S. Ouyang, J. Cao, J. Ye, Facile synthesis of rhombic dodecahedral AgX/Ag_3PO_4 (X=Cl, Br, I) heterocrystals with enhanced photocatalytic properties and stabilities, *Phys. Chem. Chem. Phys.*, **2011**, 13, 10071-10075.
[13]. G. Li, L. Mao, Maganetically separable Fe_3WO_4-Ag_3PO_4 sub micrometer composite: facile synthesis, high visible light driven photocatalysis efficiency and good recyclability, *RSC Adv.*, **2012**, 2, 5108-5111.
[14]. W. Yao, B. Zhang, C. Huang, C. Ma, X. Song, Q. X, synthesis and characterization of high efficiency and stable Ag_3PO_4/SnO_2 semiconductor nanocomposites with enhanced photocatalytic activity and stability, *New. J. Chem.*, **2012**, 36, 4050-4055.
[15]. L. Liu, J. Liu, D. D. Sun, Graphene oxide enwrapped Ag_3PO_4 composite: towards a highly efficiency and stable visible light induced photocatalyst for water purification, *Catal. Sci. Technol.*, **2012**, 2, 2525-2532.
[16]. Q. Liang, Y. Shi, W. Ma, Z. Li, X. Yang, Enhanced photocatalytic activity and structural stability by hybridizing Ag_3PO_4 nanospheres with grapheme oxide sheets, *Phys. Chem.Chem. Phys.*, **2012**, 14, 15657-15665.
[17]. Moisés I. Salazar-Gastélum, Edgar A. Reynoso-Soto, Shui W. Lin, Sergio Perez-Sicairos, Rosa M. Félix-Navarro Electrochemical and Photoelectrochemical Decoloration of Amaranth Dye Azo Using Composited Dimensional Stable Anodes, *J. Enviro. Protec.*, **2013**, 4,136-143.
[18]. V. K. Gupta, R. Jain, A. Mittal, T. A. Saleh, A. Nayak, S. Agarwal, S. Sikarwar, Photo-catalytic degradation of toxic dye amaranth on TiO_2/UV in aqueous suspensions, *Mat. Sci. Eng. C*, **2012**, 32 12–17
[19]. Chung-Hsin Wu Comparison of azo dye degradation efficiency using UV/single semiconductor and UV/coupled semiconductor systems, *Chemosphere,* **2004**, 57, 601–608.
[20]. Y. G. Su, G. S. Li, Y. F. Xue, L. P. Li, Tunable physical properties of $CaWO_4$ nanocrystal via particle size control, *J. Phys. Chem. C,* **2007**, 111 6684–6689.
[21]. M. A. Butler, Photoelectrolysis and physical properties of the semiconducting electrode WO_2, *J. Appl. Phys.*, **1977**, 48 1914–1920.
[22]. Y. P. Bi, H.Y. Hu, S. X. Ouyang, G. X. Lu, J. Y. Cao, J. H. Ye, Photocatalytic and photoelectric properties of Cubic Ag_3PO_4 submicrocrystals with shape corners and edges, *Chem. Commun.,* **2012**, 48, 3748–3750.
[23]. J. Cao, B.D. Luo, H.L. Lin, S.F. Chen, Synthesis, characterization and photocatalytic activity of AgBr/H_2WO4 composite photocatalyst, *J. Mol. Catal. A: Chem.,* **2011**, 344, 138–144.

[24]. Z. G. Yi, J. H. Ye, N. Kikugawa, T. Kako, S. Ouyang, H.S. Williams, H. Yang, J. Y. Cao, W. J. Luo, Z. S. Li, Y. Liu, R. L. Withers, An orthophosphate semiconductor with photooxidation properties under visible-light irradiation, *Nat. Mater*., **2010**, 9, 559–564.
[25]. P. Wang, B. B. Huang, X. Y. Qin, X. Y. Zhang, Y. Dai, J. Y. Wei, M.H. Whangbo, Ag@AgCl: a highly efficient and stable photocatalyst active under visible light, *Angew. Chem.*, **2008**, 47, 7931–7933.
[26]. P. Wang, B. B. Huang, X. Y. Zhang, X.Y. Qin, H. Jin, Y. Dai, Z. Y. Wang, J. Y. Wei, J. Zhan, S. Y. Wang, J.P. Wang, M. H. Wangbo, Highly efficient visible-light plasmonic photocatalyst Ag@AgBr, *Chem. Eur. J.*, **2009**, 15, 1821–1824.
[27]. Y. P. Liu, L. Fang, H. D. Lu, L. J. Liu, H. Wang, C. Z. Hu, Highly efficient and stable Ag/Ag_3PO_4 plasmonic photocatalyst in visible light, *Catal. Commun.*, **2012**, 17, 200–204.
[28]. Y. M. Moustafa, K. El-Egili, Infrared studies on the structure of sodium phosphate glasses, *J. Non-Cryst. Solids*, **1998**, 240, 144–153.
[29]. S. J. Gadaleta, E. P. Paschalis, F. Betts, R. Mendelsohn, A. L. Boskey, Fourier transform infrared spectroscopy of the solution-mediated conversion of amorphous calcium phosphate to hydroxyapatite: new correlations between X-ray diffraction and infrared data, *Calcif. Tissue Int.*, **1996**, s58, 9–16.
[30]. Ethiraj and Kang, synthesis and characterization of CuO nanowires by a simple wet chemical method, nanoscale, *Research let.*, **2012**, 7,70.
[31]. D. Paliwal, H.S. Sharma, R. Ameta, B. Kataria, Photocatalytic Degradation of Malachite Green over CuO/Al_2O_3Composite, *J. Applicable Chem*., **2018**, 7, 130-137.
[32]. A. Subalakshmi, B. Kavitha, N. Srinivasan, M. Rajarajan, A. Karthika, A. Suganthi, A Facile Novel Synthesis of Cadmium oxide Nanoparticle Decorated Oleic acid with Enhanced Photocatalytic activity for the Degradation of Crystal Violet under Solar Light Irradiation, *J. Applicable Chem*., **2019**, 8, 2348-2359.